Atomic parity violation in $0 \to 0$ two-photon transitions

D. R. Dounas-Frazer,[1,*] K. Tsigutkin,[1] D. English,[1] and D. Budker[1,2]

[1]*Department of Physics, University of California at Berkeley, Berkeley, California 94720-7300, USA*
[2]*Nuclear Science Division, Lawrence Berkeley National Laboratory, Berkeley, California 94720, USA*

(Dated: June 22, 2011)

We present a method for measuring atomic parity violation in the absence of static external electric and magnetic fields. Such measurements can be achieved by observing the interference of parity conserving and parity violating two-photon transition amplitudes between energy eigenstates of zero electronic angular momentum. General expressions for induced two-photon transition amplitudes are derived. The signal-to-noise ratio of a two-photon scheme using the $6s^2\ ^1S_0 \to 6s6p\ ^3P_0$ transition in ytterbium is estimated.

PACS numbers: 32.80.Rm, 31.30.jg

I. INTRODUCTION

High-precision measurements of parity violation in atoms, ions, and molecules constrain new physics beyond the Standard Model [1]. The processes that contribute to atomic parity violation (APV) are separated into two categories according to their dependence on nuclear spin [2]. The dominant contributions to APV usually come from nuclear spin-independent (NSI) processes, whereas nuclear spin-dependent (NSD) effects constitute small corrections. Measurements of NSI APV in cesium [3] have led to precise evaluation of the weak charge of the nucleus [4], and those of NSD APV to the first observation of the nuclear anapole moment [5]. Future APV measurements may provide information about neutron distributions [6], and may reconcile the cesium anapole measurement with the limits placed on the anapole moment in thallium [7].

APV experiments measure interference of a parity conserving transition amplitude with a parity violating one that is induced by the weak interaction [8]. Such interference leads to circular birefringence in atomic vapors, which was employed in the earliest APV observations [9–12]. Other APV experiments, including the most accurate [3] and the most recent [13], have employed the Stark-interference technique [14], a method that uses a static electric field to amplify an otherwise very small APV signal.

In addition to these well established Stark-interference techniques, there are various extensions: Light-shift measurements of amplitude interference have been proposed for various systems, including atoms [15], single trapped ions [16, 17], two-ion entangled states [18], and chiral molecules [19, 20]. The potential advantages of using electromagnetically induced transparency to measure APV-induced circular dichroism in thallium have been investigated [21]. It has also been proposed to employ interference of a parity conserving two-photon transition with a parity violating single-photon transition in cesium [22].

All these methods rely on application of static external electric and magnetic fields to amplify and discriminate APV effects. Misalignments of applied fields introduce systematic uncertainties limiting the precision of APV measurements [13]. In this work, we present a scheme for measuring NSI APV that replaces static electric and magnetic fields with optical fields that are easier to align. This scheme uses a two-photon transition between energy eigenstates with zero electronic angular momentum. Amplification of APV effects is achieved by interference of two transition amplitudes: a parity conserving amplitude describing electric-dipole-magnetic-dipole (E1-M1) transitions, and a parity violating E1-E1 amplitude. The APV signal can be discriminated from the large parity conserving background by manipulating properties of the light fields. A further advantage of this scheme is the ability to measure spurious electric and magnetic fields. This method, which we call the *all-optical scheme (AOS)*, is applicable to a variety of atomic systems.

We consider an application of the AOS that takes advantage of the large NSI APV mixing of the $6s6p\ ^1P_1$ and $5d6s\ ^3D_1$ states observed in ytterbium [13]. Precise measurements of this mixing in a chain of isotopes will provide important information about nuclear structure [23], and is a major goal of ongoing Stark-interference experiments [13]. Systematic errors due to imperfections of applied fields pose a challenge for APV experiments, and cross-checks of present and future measurements are highly valuable. In the case of cesium, for instance, a cross check was provided by a stimulated-emission experiment [24]. To this end, we propose applying the AOS to the ytterbium two-photon ($\lambda_1 = 399$ nm, $\lambda_2 = 1.28\ \mu$m) $6s^2\ ^1S_0 \to 6s6p\ ^3P_0$ transition to measure the parity-violating mixing of the intermediate $6s6p\ ^1P_1$ state with the $5d6s\ ^3D_1$ state.

From a formal point of view, the AOS is equivalent to measuring optical-rotation induced by APV on an M1 transition [25]. However, the AOS provides more field reversals compared to traditional optical-rotation experiments, thereby allowing for better discrimination of systematic effects from the APV signal. For the ytterbium system, a scheme for measuring APV-induced circular

* drdf@berkeley.edu

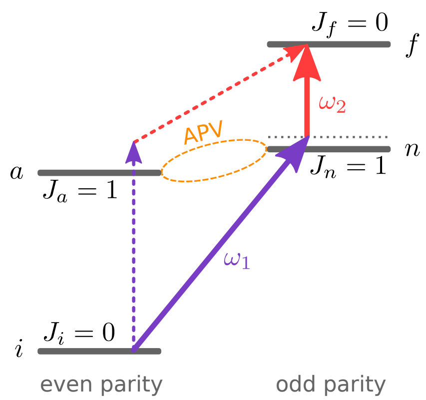

FIG. 1. (Color online) Energy levels and transitions relevant to the AOS. The dashed ellipse represents mixing of the states $|n\rangle$ and $|a\rangle$ due to the weak interaction. The dotted horizontal line represents the detuning of the light fields from the intermediate state. Thick, solid arrows and thin, dashed arrows illustrate dominant and suppressed excitation paths, respectively.

dichroism on the 1.28 μm $6s6p\ ^3P_0 \to 6s6p\ ^1P_1$ has previously been proposed [26]. The AOS has two advantages over that proposal: the light fields are cw rather than pulsed, bypassing the challenges of achieving a high repetition rate; and, circular dichroism is measured by observing population of the metastable $6s6p\ ^3P_0$ state, which allows for measurement in a region where detection conditions are easier to optimize.

II. ALL-OPTICAL SCHEME

We consider atoms illuminated by two light fields, with polarization vectors $\boldsymbol{\epsilon}_j$, propagation vectors $\mathbf{k}_j$, and frequencies ω_j, where $j = 1, 2$ is the light-field index. We denote the wavenumber $k_j \equiv |\mathbf{k}_j| = \omega_j/c$, the wavelength $\lambda_j = 2\pi/k_j$, and the field intensity $\mathcal{I}_j$. The light fields drive two-photon transitions from initial state $|i\rangle$ to final state $|f\rangle$, separated in energy by ω_{fi}. Throughout this work, we use atomic units: $\hbar = e = m_e = 1/(4\pi\varepsilon_0) = 1$. The transition rate on resonance ($\omega_1 + \omega_2 = \omega_{fi}$) is [27]:

$$R = (2\pi)^3 \alpha^2 \mathcal{I}_1 \mathcal{I}_2 |A|^2 \frac{2}{\pi \Gamma}, \tag{1}$$

where α is the fine-structure constant, A is the transition amplitude, and Γ is the width of the transition. Energy eigenstates are represented as $|i\rangle = |J_i M_i\rangle$, and likewise for $|f\rangle$. Here J_i and $M_i \in \{\pm J_i, \pm(J_i - 1), \ldots\}$ are quantum numbers associated with the electronic angular momentum and its projection along the quantization axis, respectively.

The AOS uses a two-photon transition from an initial state with $J_i = 0$ to an opposite-parity final state with $J_f = 0$. The transition is enhanced by the presence of an intermediate state $|n\rangle$ with $J_n = 1$. The character of the two-photon transition depends on the magnitude of the detuning of the light fields from the one-photon resonances involving the intermediate state [28]. When the detuning is small, the final state is populated by cascade excitation, that is, consecutive single-photon $i \to n$ and $n \to f$ transitions. We work in the opposite regime of large detuning [see condition (11) below]. In this regime, the excitation occurs via a pure two-photon transition and the population of the intermediate state is negligible.

The probability amplitude for the $i \to f$ transition has two contributions: one from a parity conserving E1-M1 transition, and another from a parity violating E1-E1 transition. The E1-E1 transition is induced by mixing of the intermediate state[1] $|n\rangle$ with opposite-parity $J = 1$ states via the weak interaction. We assume that this mixing is dominated by a single nearby state $|a\rangle$ with $J_a = 1$ (Fig. 1). The proximity of $|a\rangle$ to $|n\rangle$ leads to an M1-E1 excitation path for the $i \to f$ transition that uses the intermediate state $|a\rangle$ rather than $|n\rangle$. We incorporate the amplitude of this path into the expression for the E1-M1 amplitude below.

In the absence of stray fields, the amplitude for a two-photon $J_i = 0 \to J_f = 0$ transition is (Appendix A):

$$A = A_{\text{E1-M1}} + A_{\text{W}}, \tag{2}$$

where

$$A_{\text{E1-M1}} = [\mathcal{M}(\omega_1)\hat{\mathbf{k}}_2 - \mathcal{M}(\omega_2)\hat{\mathbf{k}}_1] \cdot (\boldsymbol{\epsilon}_1 \times \boldsymbol{\epsilon}_2) \tag{3}$$

and

$$A_{\text{W}} = i[\zeta(\omega_1) + \zeta(\omega_2)](\boldsymbol{\epsilon}_1 \cdot \boldsymbol{\epsilon}_2) \tag{4}$$

are the amplitudes corresponding to the E1-M1 and weak interaction induced E1-E1 transitions[2]. The quantities $\mathcal{M}(\omega_j)$ and $\zeta(\omega_j)$ are

$$\mathcal{M}(\omega_j) = \frac{1}{3}\left(\frac{\mu_{fn}\, d_{ni}}{\omega_{ni} - \omega_j} + \frac{d_{fa}\, \mu_{ai}}{\omega_{ai} - \omega_j}\right) \tag{5}$$

and

$$\zeta(\omega_j) = \frac{1}{3}\frac{d_{fa}\, \Omega_{an}\, d_{ni}}{\omega_{na}}\left(\frac{1}{\omega_{ni} - \omega_j} - \frac{1}{\omega_{ai} - \omega_j}\right), \tag{6}$$

where μ_{fn} and d_{ni} are the reduced matrix elements of the magnetic- and electric-dipole moments, respectively.

[1] Alternatively, the E1-E1 transition could be induced by mixing of the final state $|f\rangle$ with a nearby opposite-parity $J = 0$ state. Such a scheme is equivalent to the AOS, and shares the key features of the AOS presented in this work.

[2] The E1-M1 amplitude is a product of the matrix elements of the operators describing E1 and M1 single-photon transitions. Because the E1 (M1) operator is odd (even) under spatial inversion, the E1-M1 amplitude is a pseudoscalar. A similar argument shows that the E1-E1 amplitude is a normal scalar.

Here ω_{na} is the energy splitting of states $|a\rangle$ and $|n\rangle$, and Ω_{an} is the magnitude of the reduced matrix element of the NSI APV Hamiltonian $H_{\rm W}$ [see Eq. (A7) in the Appendix].

The two terms in Eqs. (5, 6) correspond to the two different excitation paths for the transition. When states $|n\rangle$ and $|a\rangle$ are perfectly degenerate ($\omega_{na}=0$), the induced E1-E1 paths interfere destructively and the parity violating amplitude vanishes. We limit our discussion to atomic systems for which ω_{na} is sufficiently large that one path is dominant. We assume that $\Delta=\omega_1-\omega_{ni}$ is much smaller than all other detunings from the intermediate states $|n\rangle$ and $|a\rangle$. In this case, only

$$\mathcal{M}(\omega_1)\approx\mathcal{M}\equiv\frac{1}{3}\frac{\mu_{fn}\,d_{ni}}{\Delta} \tag{7}$$

and

$$\zeta(\omega_1)\approx\zeta\equiv\frac{1}{3}\frac{d_{fa}\,\Omega_{an}\,d_{ni}}{\omega_{na}\Delta} \tag{8}$$

contribute significantly to Eqs. (3, 4). Because $\mathcal{M}$ and ζ have the same complex phase [2], the relative phase between $A_{\text{E1-M1}}$ and $A_{\rm W}$ is determined by the field geometry. Hereafter, we assume that $\mathcal{M}$ and ζ are real parameters since their common phase is arbitrary.

The goal of the AOS is to observe interference of amplitudes $A_{\rm W}$ and $A_{\text{E1-M1}}$ in the rate R. As Eqs. (1-4) show, R consists of a large parity conserving term proportional to $\mathcal{M}^2$, a small parity violating term (the interference term) proportional to $\mathcal{M}\zeta$, and a negligibly small term on the order of ζ^2. The interference term is proportional to a pseudoscalar quantity that depends only on the field geometry, the *rotational invariant*:

$$\mathrm{Im}\{(\boldsymbol{\epsilon}_1\cdot\boldsymbol{\epsilon}_2)^*[(\boldsymbol{\epsilon}_1\times\boldsymbol{\epsilon}_2)\cdot\mathbf{k}_2]\}, \tag{9}$$

which is odd under parity reversal (P-odd) and even under time reversal (T-even)[3]. The time reversal invariance of expression (9) can be understood in the following way. Time reversal requires that initial and final states be interchanged, which corresponds to complex conjugation. The imaginary part of a complex number is therefore T-odd. Since the photon momentum $\mathbf{k}_2$ is also T-odd, the rotational invariant (9) is T-even.

Restrictions on the geometry of the light fields are inferred from the form of the rotational invariant. The rotational invariant–and hence the interference term–vanishes for plane polarized light beams. One way to achieve a nonzero rotational invariant is to choose circular polarization for the second beam: $\boldsymbol{\epsilon}_2=\boldsymbol{\sigma}_\pm$, where we have assumed $\mathbf{k}_2$ lies along the z axis. For arbitrary polarization $\boldsymbol{\epsilon}_1=a_+\boldsymbol{\sigma}_++a_-\boldsymbol{\sigma}_-$ of the first beam, conservation of angular momentum requires that only the polarization component $a_\mp$ contributes to the excitation process. Thus the rotational invariant (9) reduces to $\pm|a_\mp|^2k_z$, where $k_z=+1$ ($k_z=-1$) when $\mathbf{k}_2$ is aligned (anti-aligned) with the z-axis.

For two collinear circularly polarized beams of light oriented along the z-axis, the transition rate is

$$R\propto|A|^2=\mathcal{M}^2\pm2k_z\mathcal{M}\zeta, \tag{10}$$

where the positive (negative) sign in Eq. (10) is taken when beam 2 has $\boldsymbol{\sigma}_+$ ($\boldsymbol{\sigma}_-$) polarization. The interference term is discriminated from the total transition rate either by reversing the direction of the propagation vector $\mathbf{k}_2$, or by reversing the sense of rotation of the circularly polarized light fields. The asymmetry $2\zeta/\mathcal{M}=2(d_{fa}/\mu_{fn})(\Omega_{an}/\omega_{na})$ is obtained by dividing the difference of rates upon a reversal by their sum.

We propose to measure the transition rate by probing the population of the final state $|f\rangle$, and assume that the following conditions are met: (i) detuning of the light fields from the intermediate state is large enough to realize a pure two-photon transition, and (ii) light intensities are low enough that the transition is not saturated. A pure two-photon transition is achieved when [27, 28]

$$|\Delta|\gg\Omega_0, \tag{11}$$

where

$$\Omega_0=\sqrt{\frac{8\pi\alpha}{3}\Big(d_{ni}^2\,\mathcal{I}_1+\mu_{fn}^2\,\mathcal{I}_2\Big)} \tag{12}$$

is the interaction energy. When condition (11) is satisfied, the system reduces to a two-level system consisting of the initial and final states coupled by an effective optical field. Saturation effects can be ignored when the pumping rate R is much smaller than the relaxation rate Γ' of the final state, that is, when

$$\mathcal{I}_1\mathcal{I}_2\ll\left[\frac{3}{\pi\alpha}\frac{\Delta}{d_{ni}\,\mu_{fn}}\right]^2\Gamma\Gamma'. \tag{13}$$

In this regime, the population of the final state is proportional to the rate given by Eq. (1).

The shot-noise limited sensitivity of the AOS is estimated as follows. The probe signal is proportional to the number of excited atoms. The number of excited atoms associated with the parity violating part of the transition rate is

$$N=[(4\pi\alpha)^2\mathcal{I}_1\mathcal{I}_2(2\mathcal{M}\zeta)/\Gamma]N_it, \tag{14}$$

where t is the effective integration time of the measurement and N_i is the total number of atoms initially in state $|i\rangle$. The measurement noise is given by $\delta N=\sqrt{N'}$, where

$$N'=[(4\pi\alpha)^2\mathcal{I}_1\mathcal{I}_2\mathcal{M}^2/\Gamma]N_it \tag{15}$$

[3] The rotational invariant presented in Eq. (9) is not symmetric under photon exchange because we have neglected the terms proportional to $\mathcal{M}(\omega_2)$ and $\zeta(\omega_2)$ in Eqs. (3, 4). When these terms are included, R has two interference terms whose sum is exchange symmetric. In the case of degenerate photons ($\omega_1=\omega_2$), the sum of the interference terms is proportional to the exchange symmetric rotational invariant $\mathrm{Im}\{(\boldsymbol{\epsilon}_1\cdot\boldsymbol{\epsilon}_2)^*[(\boldsymbol{\epsilon}_1\times\boldsymbol{\epsilon}_2)\cdot(\hat{\mathbf{k}}_1-\hat{\mathbf{k}}_2)]\}$.

is the number of excited atoms associated with the parity conserving part of the transition rate. The signal-to-noise ratio (SNR) of the probe signal is $N/\delta N$, or

$$\mathrm{SNR} = \frac{8\,\pi\alpha}{3}\,\frac{d_{fa}\,\Omega_{an}\,d_{ni}}{\omega_{na}|\Delta|}\sqrt{\frac{\mathcal{I}_1\,\mathcal{I}_2\,N_i\,t}{\Gamma}}. \tag{16}$$

As expected, the SNR increases for large Ω_{an} and high light intensities. Although purely statistical shot-noise dominated SNR does not contain μ_{fn}, this amplitude is still an important parameter in practice due to conditions (11, 13). Large μ_{fn} leads to small APV asymmetry which requires better control over experimental parameters (see Sec. III). In the opposite case of small μ_{fn}, an observable signal requires high light intensities which may pose a technical challenge.

Although we have focused on a ladder-type three-level atomic system (Fig. 1), the discussion presented here holds for lamda-type systems (Fig. 2) as well. However, the following modifications must be made: In a lambda-type system, the polarization of the absorbed photon $\boldsymbol{\epsilon}_2$ is replaced by the polarization of the photon emitted by stimulated emission. Consequently, conservation of energy requires that the two-photon resonance condition above Eq. (1) becomes $\omega_1 - \omega_2 = \omega_{fi}$, and conservation of angular momentum requires that both circularly polarized beams have the same sense of rotation. Then the positive (negative) sign is taken in Eq. (10) when $\boldsymbol{\epsilon}_1 = \boldsymbol{\epsilon}_2 = \sigma_{-(+)}$.

III. PARASITIC SOURCES OF ASYMMETRY

Systematic effects may also contribute to the asymmetry and mask the APV signal. In this section, we discuss three potential sources of such parasitic asymmetry: imperfections of applied optical fields; Stark interference due to stray electric fields, and; shifts of the intermediate state energy induced by external fields.

A. Optical field imperfections

To understand the effects of imperfections in the optical fields, we relax the assumptions of collinear light beams and perfectly circular polarization. Beam misalignment is characterized by the angle $\theta \ll 1$ between $\mathbf{k}_2$ and $\mathbf{k}_1$. We choose the z-axis to lie along $\mathbf{k}_2$ so that θ is the polar angle of $\mathbf{k}_1$. Deviations from circular polarization are characterized by the parameters $\eta_j \ll 1$. Here $|\varphi_j| = \pi/4 - \eta_j$ is the magnitude of the ellipticity[4] of the jth beam.

Field imperfections lead to additional parity conserving terms[5] in R on the order of $\mathcal{M}^2[\theta^2/2 + (\eta_1+\eta_2)^2]$. Although these corrections to R do not mimic APV, they nevertheless contribute to the asymmetry if they change upon reversal. To simplify our analysis, we assume that changes inθ and η_j between reversals are on the order of θ and η_j for any particular reversal. We further assume that η_1 and η_2 are the same order of magnitude: $\eta_1 \simeq \eta_2 \equiv \eta$. Then spurious ellipticity and beam misalignment give rise to a parasitic asymmetry on the order of $\theta^2 + 2\eta^2$, and may mask the APV signal if they are large. Asymmetry due to field imperfections is negligible compared to APV asymmetry when

$$\theta^2 \ll 2\zeta/\mathcal{M} \quad \text{and} \quad \eta^2 \ll \zeta/\mathcal{M}. \tag{17}$$

B. Stark interference

The derivation of Eq. (10) assumes the absence of external fields. Here we relax this assumption and discuss the uncertainty in the AOS that arises due to spurious electric fields. In the presence of a static electric field $\mathbf{E}$, Stark mixing of $|n\rangle$ and $|a\rangle$ induces an E1-E1 transition between the initial and final states. The Stark-induced transition amplitude is (Appendix A):

$$A_{\mathrm{S}} = i\xi[\mathbf{E}\cdot(\boldsymbol{\epsilon}_1\times\boldsymbol{\epsilon}_2)], \tag{18}$$

where

$$\xi = \frac{1}{3\sqrt{6}}\,\frac{d_{fa}\,d_{an}\,d_{ni}}{\omega_{na}\Delta}. \tag{19}$$

After including the effects of stray fields and misalignments, the transition rate (10) becomes

$$R \propto \mathcal{M}^2 + \xi^2 E_z E_1 \pm k_z\big(\mathcal{M}\xi E_\perp + 2\mathcal{M}\zeta\big), \tag{20}$$

where E_z is the z component of the electric field, $E_1 = \mathbf{E}\cdot\hat{\mathbf{k}}_1 \approx E_z$, $E_\perp = |\mathbf{E}\cdot(\hat{\mathbf{k}}_1\times\hat{\mathbf{k}}_2)| \lesssim \theta|\mathbf{E}|$, and only terms linear in θ and η_j are presented. The terms in the parentheses represent the combined effects of APV and Stark interference. These interference terms exhibit the same behavior under reversals of the light fields. This means that there is a contribution to the asymmetry on the order of $\theta\xi E/\mathcal{M}$, where E is the magnitude of $|\mathbf{E}|$. APV asymmetry dominates over asymmetry due to Stark interference when

$$E \ll 2\zeta/(\theta\xi). \tag{21}$$

---

[4] The polarization $\boldsymbol{\epsilon}_j$ of arbitrarily polarized light is parameterized in terms of the polarization angle ϑ_j and the ellipticity φ_j in the following way: $\boldsymbol{\epsilon}_j = (\cos\vartheta_j\cos\varphi_j - i\sin\vartheta_j\sin\varphi_j)\mathbf{e}_x + (\sin\vartheta_j\cos\varphi_j + i\cos\vartheta_j\sin\varphi_j)\mathbf{e}_y$. Linearly, circularly, and elliptically polarized light are described by $\varphi_j = 0$, $|\varphi_j| = \pi/4$ and $0 < |\varphi_j| < \pi/4$, respectively. The sense of rotation is determined by the relative sign of the real and imaginary parts of $\boldsymbol{\epsilon}_j$: $\boldsymbol{\epsilon}_j = \boldsymbol{\sigma}_\pm$ when $\varphi_j = \pm\pi/4$.

[5] Beam misalignment is further characterized by the azimuthal angle ϕ of $\mathbf{k}_1$. Taking this into account, the transition rate becomes $R \to R - \mathcal{M}^2[\theta^2/2 + \eta_1^2 + \eta_2^2 + 2\eta_1\eta_2\cos(2\vartheta - 2\phi)]$, where $\vartheta = \vartheta_2 - \vartheta_1$ is the relative polarization angle of the light fields. In the text we treat the case of maximal correction, that is, $\vartheta = \phi$.

C. Energy shifts of the intermediate state

The transition rate must be further modified to account for light shifts and effects of stray magnetic fields. We consider energy shifts of the form $M_n^2\delta_2 + M_n\delta_1$, where M_n is the magnetic quantum number of $|n\rangle$. The parameter δ_2 is due to tensor shifts caused by the light fields or dc electric fields. We neglect quadratic Zeeman shifts that arise in the presence of transverse magnetic fields. In general, many levels may contribute to light shifts of the intermediate state. We approximate light shifts by their contributions from the initial and final states. Then the light shifts are approximately equal to $\Omega_0^2/(4\Delta)$, where Ω_0 is given by Eq. (12). When the dc polarizability of the intermediate state is dominated by Stark mixing of $|n\rangle$ and $|a\rangle$, dc Stark shifts of that state are on the order of $d_{an}^2E^2/(2\omega_{na})$. Then

$$\delta_2 \approx \Omega_0^2/(4\Delta) + d_{an}^2E^2/(2\omega_{na}). \quad (22)$$

On the other hand, the parameter δ_1 is due to vector light shifts and the dc Zeeman effect. Vector light shifts change sign upon reversal of circular polarization ($\boldsymbol{\sigma}_\pm \to \boldsymbol{\sigma}_\mp$). In this case,

$$\delta_1 \approx \pm\Omega_0^2/(4\Delta) + g\mu_0 B, \quad (23)$$

where g is the Landé factor of the intermediate state, B is the magnitude of the stray magnetic field, and $g\mu_0 B$ is the order of magnitude of the Zeeman shift.

The corrected E1-M1 and Stark-induced E1-E1 transition amplitudes are obtained by expanding the energy denominators in Eqs. (5, 19) to first order in $\delta_{1,2}$. Corrections to the weak interaction induced amplitude (6) are neglected here. The transition rate is

$$R \propto \mathcal{M}^2\left[1 + 2(\delta_2 \pm \delta_1)/\Delta\right] + \xi^2 E_1 E_z - \\ - 2\xi^2 E_z^2(\delta_2 \pm \delta_1)/\Delta \pm k_z\left(\mathcal{M}\xi E_\perp + 2\mathcal{M}\zeta\right), \quad (24)$$

where summation over the magnetic sublevels of $|n\rangle$ has been taken into account. Only the Stark interference term $\mathcal{M}\xi E_\perp$ has the same signature as APV. The Stark and Zeeman shift corrections can be discriminated from the other terms in Eq. (24) by changing the sign of Δ, and can be discriminated from each other by reversing the sense of rotation of the circularly polarized light fields. Thus stray electric and magnetic fields can be measured by alternating the sign of the detuning of the light fields from the intermediate state.

IV. APPLICATIONS TO YTTERBIUM

We now turn our attention to the two-photon $6s^2\ {}^1S_0 \to 6s6p\ {}^3P_0$ transition in ytterbium. This transition can be driven by two light fields of wavelengths $\lambda_1 = 399$ nm and $\lambda_2 = 1.28\ \mu$m, which are nearly resonant with transitions involving the intermediate $6s6p\ {}^1P_1$ state (Fig. 2). The parity violating E1-E1 transition is induced by the mixing of the $6s6p\ {}^1P_1$ and $5d6s\ {}^3D_1$ states due to the weak interaction. This mixing arises because $6s6p\ {}^1P_1$ has a large admixture of the configuration $5d6p$ [32, 33]. The parameter describing mixing of $6s6p\ {}^1P_1$ and $5d6s\ {}^3D_1$ was measured to be $\Omega_{an}/\omega_{na} = 6\times10^{-10}$ [13]. Other essential atomic parameters are given in Table I. The ytterbium system is characterized by the asymmetry $2\zeta/\mathcal{M} \approx 6\times10^{-6}$, which is more than an order of magnitude larger than asymmetries measured in optical-rotation experiments in bismuth, lead, and thallium [1].

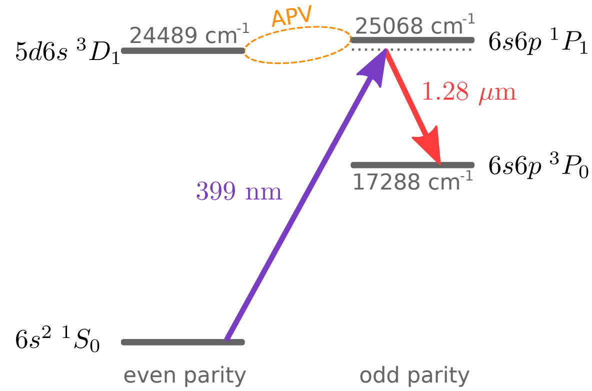

FIG. 2. (Color online) Application of AOS to ytterbium.

TABLE I. Atomic data for application of AOS to ytterbium. Here a_0 and μ_0 are the Bohr radius and magneton.

	Transition ($1 \to 2$)	$d_{21}/(ea_0)$	μ_{21}/μ_0
	$6s^2\ {}^1S_0 \to 6s6p\ {}^1P_1$	4.1[a]	
E1	$6s6p\ {}^3P_0 \to 5d6s\ {}^3D_1$	2.6[b]	
	$5d6s\ {}^3D_1 \to 6s6p\ {}^1P_1$	0.27[b]	
M1	$6s^2\ {}^1S_0 \to 5d6s\ {}^3D_1$		1.33[c] $\times 10^{-4}$
	$6s6p\ {}^3P_0 \to 6s6p\ {}^1P_1$		0.13[d]

[a] Ref. [29]
[b] Ref. [30]
[c] Ref. [31]
[d] Ref. [26]

For concreteness, we consider a hypothetical experiment using an atomic beam similar to that of Ref. [13]: characteristic thermal speed 3×10^4 cm/s, density 2×10^9 cm^{-3}, radius 1 cm. The atomic beam intersects two overlapping, collinear laser beams where atoms interact with the 399 nm and 1.28 μm light and undergo the $6s^2\ {}^1S_0 \to 6s6p\ {}^3P_0$ transition. High light powers–which are necessary to achieve a large SNR–can be realized using a unidirectional ring cavity. The transition rate can be measured by probing the population of the metastable $6s6p\ {}^3P_0$ state using the detection method described in Ref. [13].

To estimate the SNR, we choose light parameters that satisfy conditions (11, 13). The laser beams have a Guassian profile with a characteristic radius of 2 mm, and the frequencies are detuned from the intermediate state by $\Delta = 2\pi \times 800$ MHz, about 30 times larger than the width of the intermediate state. In the interaction region, the metastable state acquires a radiative decay rate on the order of $\Gamma' = [\Omega_0^2/(4\Delta^2)]\tau^{-1} = 2\pi \times 30$ kHz, where $\tau = 5.68$ ns is the lifetime of $6s6p\ ^1P_1$ [29]. The width of the $6s^2\ ^1S_0 \to 6s6p\ ^3P_0$ transition is dominated by the transit-broadened linewidth[6] $\Gamma = 2\pi \times 90$ kHz. For light powers of 10 W at 1.28-μm and 10 mW at 399-nm, Eq. (16) gives SNR $\approx 2\sqrt{t(\mathrm{s})}$. Based on these estimates, a one-hour measurement may achieve better than 1% statistical uncertainty in determination of parity violation.

Parasitic asymmetry due to field imperfections and stray electric fields can be controlled by aligning the laser beams over a large distance. In order to limit asymmetry due to beam misalignment to less than 1% of the APV asymmetry, the angle between the nominally collinear laser beams must be controlled to better than one-tenth of a beam radius of transverse displacement over a distance of one meter, which corresponds to a beam misalingment of 0.01°. Similarly, the deviation from circular polarization must also be smaller than about 0.01°. In this case, the systematic uncertainty due to Stark interference effects is below 1% for electric fields smaller than 8 V/cm. In Ref. [13], stray electric fields were measured to be on the order of 1 V/cm. In that experiment, stray electric fields are partially attributed to charge buildup on surfaces of electrodes and coils that are used to generate external static electric and magnetic fields. For the AOS, the absence of such surfaces will likely result in even smaller stray fields.

It is important to consider other mechanisms for population of the metastable $6s6p\ ^3P_0$ state, causing background and noise. The metastable state may be populated by multiphoton processes involving highly excited states, or by molecular processes in the presence of dimers or other molecular impurities in the atomic beam. These detrimental effects will contribute to a background that dependends on Δ, compromising the search for stray fields [25]. We note that no evidence of molecular impurities has been seen in the Yb APV epxeriments up to date [13].

To better understand the feasibility of the proposed experiment, we compare the predicted SNR of the two-photon AOS to the observed SNR of the one-photon Stark-interference experiment [13]. This comparison is especially relevant since both techniques employ the same method for probing the population of the metastable $6s6p\ ^3P_0$ state in ytterbium. The shot-noise limited SNR in Ref. [13] was demonstrated to be $2\sqrt{t(\mathrm{s})}$. However, the Stark-interference experiment is not currently shot-noise limited; the measurement uncertainty is determined by systematic effects due to imperfections of applied fields. Because the AOS has similar projected statistical sensitivity and possibly better control of systematics compared to the Stark-interference experiment, the AOS is an attractive candidate for future APV measurements in ytterbium.

[6] The transit-broadened width of a one-photon transition is $\Gamma_0 \approx 2.4v/r$ [34], where v is the atomic velocity and r is the $1/e$ radius of the light electric field profile. The matrix element for a two-photon transition is proportional to the product of the two light electric fields, and hence to the product of their Gaussian profiles [27]. Therefore, the transit-broadened width is $\Gamma = \sqrt{2}\Gamma_0$ when the beam profiles are identical.

V. SUMMARY AND DISCUSSION

A scheme for measuring APV using interference of parity conserving E1-M1 and parity violating E1-E1 two-photon transition amplitudes was presented. The AOS allows for observations of NSI APV in the absence of external static electric and magnetic fields. This method measures the rate of a transition between two energy eigenstates with zero total electronic angular momentum. General expressions for the two-photon transition rate and SNR were derived. Because the AOS uses optical fields rather than static electric and magnetic fields, systematic effects due to field misalignments are easier to minimize in the AOS than in ongoing APV measurements [13].

To demonstrate the feasibility of the AOS, we estimated the SNR of the $6s^2\ ^1S_0 \to 6s6p\ ^3P_0$ transition in ytterbium ($\lambda_1 = 399$ nm, $\lambda_2 = 1.28\ \mu$m). Our estimate of the SNR suggests that this system is a promising candidate for a cross-check of recent APV measurements in ytterbium [13], and future measurements of APV in a chain of isotopes. While we considered atoms with zero nuclear spin, the AOS could also be applied to isotopes with nonzero nuclear spin provided that the detuning Δ is much larger than the hyperfine splitting of the intermediate state.

Another candidate for the AOS is the ladder-type $4f^66s^2\ ^7F_0 \to 4f^66s6p\ ^7F_0$ transition ($\lambda_1 = 639$ nm, $\lambda_2 = 1.56\ \mu$m) in samarium. The E1-E1 transition is induced by mixing of the opposite-parity states $4f^65d6s\ ^7G_1$ and $4f^66s6p\ ^7G_1$ due to the weak interaction. The APV effect in samarium is expected to be of the same order of magnitude as that observed in ytterbium [35]. A version of the AOS that uses photons of the same frequency has been previously suggested in a proposal for a search for APV using the 1 μm $1s2p\ ^3P_0 \to 1s2s\ ^1S_0$ transition in uranium ions [36]. However, the uranium-ion experiment is not currently feasible because the required laser intensity is on the order of 10^{21} W/cm^2.

VI. ACKNOWLEDGEMENTS

The authors acknowledge helpful discussions with M. A. Bouchiat, A. Cingöz, M. Kozlov, N. A. Leefer, and J. Stalnaker. This work has been supported by NSF.

Appendix A: Two-photon transition amplitudes

In this section, we derive amplitudes for E1-M1 and induced E1-E1 $J_i = 0 \to J_f = 0$ transitions. We use the following convention for the Wigner-Eckart theorem (WET). Let T_k be an irreducible tensor of rank k with spherical components T_{kq} for $q \in \{0, \pm 1, \ldots, \pm k\}$. Then the WET is [37]

$$\langle J_2 M_2 | T_{kq} | J_1 M_1 \rangle = (J_2 || T_k || J_1) \frac{\langle J_1 M_1; kq | J_2 M_2 \rangle}{\sqrt{2J_2 + 1}}, \tag{A1}$$

where $(J_2||T_k||J_1)$ is the reduced matrix element of T_k and $\langle J_1 M_1; kq|J_2 M_2\rangle$ is a Clebsch-Gordan coefficient.

The amplitude for the E1-M1 transition is [27]

$$\begin{aligned} A_{\text{E1-M1}} = A_{\text{E1-M1}}(1,2) + A_{\text{E1-M1}}(2,1) \\ + A_{\text{M1-E1}}(1,2) + A_{\text{M1-E1}}(2,1), \end{aligned} \tag{A2}$$

where

$$A_{\text{E1-M1}}(j,j') = \langle f | (\hat{\mathbf{k}}_{j'} \times \boldsymbol{\epsilon}_{j'}) \cdot \boldsymbol{\mu} \, \frac{|n\rangle\langle n|}{\omega_{ni} - \omega_j} \, \boldsymbol{\epsilon}_j \cdot \mathbf{d} | i \rangle, \tag{A3}$$

and

$$A_{\text{M1-E1}}(j,j') = \langle f | \boldsymbol{\epsilon}_{j'} \cdot \mathbf{d} \, \frac{|a\rangle\langle a|}{\omega_{ai} - \omega_j} \, (\hat{\mathbf{k}}_j \times \boldsymbol{\epsilon}_j) \cdot \boldsymbol{\mu} | i \rangle, \tag{A4}$$

for $j, j' = 1, 2$. Here $\boldsymbol{\mu}$ and $\mathbf{d}$ are the magnetic- and electric-dipole moments of the atom, and summation over the magnetic sublevels of the intermediate states $|n\rangle$ and $|a\rangle$ is implied.

E1-E1 transitions are induced by mixing of the states $|n\rangle$ and $|a\rangle$ due to the weak interaction and, in the presence of a static electric field, the Stark effect. The perturbed states $|n\rangle + \chi|a\rangle$ and $|a\rangle - \chi^*|n\rangle$ act as intermediate states for the two paths that contribute to the induced E1-E1 amplitude. Here χ is a small dimensionless parameter that depends on the details of the perturbing Hamiltonian. The amplitude for the induced E1-E1 transition is [27]

$$A_{\text{E1-E1}} = A_{\text{E1-E1}}(1,2) + A_{\text{E1-E1}}(2,1), \tag{A5}$$

where

$$A_{\text{E1-E1}}(j,j') = \langle f | \boldsymbol{\epsilon}_{j'} \cdot \mathbf{d} \left[\frac{\chi |a\rangle\langle n|}{\omega_{ni} - \omega_j} - \frac{|a\rangle\langle n| \chi}{\omega_{ai} - \omega_j} \right] \boldsymbol{\epsilon}_j \cdot \mathbf{d} | i \rangle. \tag{A6}$$

Like for Eqs. (A3, A4), summation over the magnetic sublevels of states $|n\rangle$ and $|a\rangle$ is implied.

When the mixing of $|n\rangle$ and $|a\rangle$ is due to the weak interaction alone, the perturbation parameter is given by $\chi = \chi_{\text{W}}$ where

$$\chi_{\text{W}} = \frac{\langle a | H_{\text{W}} | n \rangle}{\omega_{na}} = \frac{i}{\sqrt{3}} \frac{\Omega_{an}}{\omega_{na}}, \tag{A7}$$

for $J_a = J_n$ and $M_a = M_n$. Here Ω_{an} is a real parameter related to the reduced matrix element of H_{W} by $(J_a||H_{\text{W}}||J_n) = i\Omega_{an}$. The factor of i preserves time reversal invariance [2].

In the presence of a static electric field $\mathbf{E}$, the perturbation parameter becomes $\chi = \chi_{\text{W}} + \chi_{\text{S}}$, where χ_{W} is given by Eq. (A7) and

$$\chi_{\text{S}} = \frac{\langle a | H_{\text{S}} | n \rangle}{\omega_{na}} = -\frac{d_{an} E_q^*}{\omega_{na}} \frac{\langle J_n M_n; 1q | J_a M_a \rangle}{\sqrt{2J_a + 1}}, \tag{A8}$$

where d_{an} is the reduced matrix element of the electric-dipole operator. Here $H_{\text{S}} = -\mathbf{d} \cdot \mathbf{E}$ is the Stark Hamiltonian, E_q is the qth spherical component of $\mathbf{E}$, $E_q^* = (-1)^q E_{-q}$, and $q = M_a - M_n$. In this case, $A_{\text{E1-E1}} = A_{\text{W}} + A_{\text{S}}$, where $A_{\text{W}} \propto \chi_{\text{W}}$ and $A_{\text{S}} \propto \chi_{\text{S}}$ are the amplitudes of the transitions induced by the weak interaction and Stark effect, respectively.

For a general $J_i \to J_f$ transition, the Stark-induced E1-E1 amplitude may have contributions from each of the irreducible tensors that can be formed by the three vectors $\boldsymbol{\epsilon}_1$, $\boldsymbol{\epsilon}_2$, and $\mathbf{E}$. There are seven such tensors: one of rank 0, three of rank 1, two of rank 2, and one of rank 3. However, for a $J_i = 0 \to J_f = 0$ transition, only the rank-0 tensor contributes. This tensor is [38]

$$\begin{aligned} T_{00} &= \sum_{\lambda,q} \langle 1\lambda; 1q | 00 \rangle \{\boldsymbol{\epsilon}_1 \otimes \boldsymbol{\epsilon}_2\}_{1\lambda} E_q \\ &= -\frac{i}{\sqrt{6}} \mathbf{E} \cdot (\boldsymbol{\epsilon}_1 \times \boldsymbol{\epsilon}_2), \end{aligned} \tag{A9}$$

where

$$\begin{aligned} \{\boldsymbol{\epsilon}_1 \otimes \boldsymbol{\epsilon}_2\}_{1\lambda} &= \sum_{\mu,\nu} \langle 1\mu; 1\nu | 1\lambda \rangle \epsilon_{1\mu} \epsilon_{2\nu} \\ &= \frac{i}{\sqrt{2}} (\boldsymbol{\epsilon}_1 \times \boldsymbol{\epsilon}_2)_\lambda \end{aligned} \tag{A10}$$

is the irreducible tensor of rank 1 formed by $\boldsymbol{\epsilon}_1$ and $\boldsymbol{\epsilon}_2$. Here $\lambda,\ q,\ \mu,\ \nu = 0,\ \pm 1$ are the spherical components of $\{\boldsymbol{\epsilon}_1 \otimes \boldsymbol{\epsilon}_2\}_1$, $\mathbf{E}$, $\boldsymbol{\epsilon}_1$, and $\boldsymbol{\epsilon}_2$, respectively. The Stark-induced transition amplitude is

$$A_{\text{S}} = i[\xi(\omega_1) - \xi(\omega_2)][\mathbf{E} \cdot (\boldsymbol{\epsilon}_1 \times \boldsymbol{\epsilon}_2)]. \tag{A11}$$

The coefficient $\xi(\omega_j)$ can be expressed in terms of reduced electric-dipole matrix elements by applying the WET to Eq. (A5) with $\chi = \chi_{\text{S}}$ and comparing the result to Eq. (A11). This procedure yields

$$\xi(\omega_j) = \frac{1}{3\sqrt{6}} \frac{d_{fa}\, d_{an}\, d_{ni}}{\omega_{na}} \left(\frac{1}{\omega_{ni} - \omega_j} - \frac{1}{\omega_{ai} - \omega_j} \right). \tag{A12}$$

The Stark effect may also cause the final state $|f\rangle$ to mix with nearby opposite-parity $J = 1$ states. In this case, Eq. (A11) is still valid, but Eq. (A12) must be modified to account for additional admixtures of states.

Expressions (3, 4) for the amplitudes of the E1-M1 and weak interaction-induced E1-E1 transitions are derived by direct application of the WET to Eqs. (A2, A5). The Stark-induced E1-E1 amplitude in Eq. (A11) reduces to expression (18) when $|\Delta| \ll |\omega_{na}|$ and $|\Delta| \ll |\omega_2 - \omega_{ni}|$.

[1] J. S. M. Ginges and V. V. Flambaum, Phys. Rep. **397**, 63 (2004).
[2] I. B. Khriplovich, *Parity Nonconservation in Atomic Phenomena* (Gordon and Breach Science Publishers S.A., 1991).
[3] C. S. Wood, S. C. Bennett, D. Cho, B. P. Masterson, J. L. Roberts, C. E. Tanner, and C. E. Wieman, Science **275**, 1759 (1997).
[4] S. G. Porsev, K. Beloy, and A. Derevianko, Phys. Rev. Lett. **102**, 181601 (2009).
[5] V. V. Flambaum and D. W. Murray, Phys. Rev. C **56**, 1641 (1997).
[6] C. J. Horowitz, S. J. Pollock, P. A. Souder, and R. Michaels, Phys. Rev. C **63**, 025501 (2001).
[7] P. A. Vetter, D. M. Meekhof, P. K. Majumder, S. K. Lamoreaux, and E. N. Fortson, Phys. Rev. Lett. **74**, 2658 (1995).
[8] J. Guéna, M. Lintz, and M.-A. Bouchiat, Mod. Phys. Lett. A **20**, 375 (2005).
[9] L. M. Barkov and M. S. Zolotarev, Pis'ma Zh. Eksp. Teor. Fiz **28**, 544 (1978).
[10] Y. V. Bogdanov, I. I. Sobelman, V. N. Sorokin, and I. I. Struk, JETP Letters **31**, 214 (1980).
[11] M. J. D. Macpherson, K. P. Zetie, R. B. Warrington, D. N. Stacey, and J. P. Hoare, Phys. Rev. Lett. **67**, 2784 (1991).
[12] D. M. Meekhof, P. A. Vetter, P. K. Majumder, S. K. Lamoreaux, and E. N. Fortson, Phys. Rev. A **52**, 1895 (1995).
[13] K. Tsigutkin, D. Dounas-Frazer, A. Family, J. E. Stalnaker, V. V. Yashchuk, and D. Budker, Phys. Rev. Lett. **103**, 071601 (2009); Phys. Rev. A **81**, 032114 (2010).
[14] M. A. Bouchiat and C. Bouchiat, Journal de Physique **35**, 899 (1974); **36**, 493 (1975).
[15] M.-A. Bouchiat, Phys. Rev. Lett. **100**, 123003 (2008).
[16] N. Fortson, Phys. Rev. Lett. **70**, 2383 (1993).
[17] L. W. Wansbeek, B. K. Sahoo, R. G. E. Timmermans, K. Jungmann, B. P. Das, and D. Mukherjee, Phys. Rev. A **78**, 050501 (2008).
[18] P. Mandal and M. Mukherjee, Phys. Rev. A **82**, 050101 (2010).
[19] R. A. Harris and L. Stodolsky, Physics Letters B **78**, 313 (1978).
[20] P. Bargueño, I. Gonzalo, and R. Pérez de Tudela, Phys. Rev. A **80**, 012110 (2009).
[21] A. D. Cronin, R. B. Warrington, S. K. Lamoreaux, and E. N. Fortson, Phys. Rev. Lett. **80**, 3719 (1998).
[22] M. Gunawardena and D. S. Elliott, Phys. Rev. Lett. **98**, 043001 (2007); Phys. Rev. A **76**, 033412 (2007).
[23] B. A. Brown, A. Derevianko, and V. V. Flambaum, Phys. Rev. C **79**, 035501 (2009).
[24] J. Guéna, D. Chauvat, P. Jacquier, E. Jahier, M. Lintz, S. Sanguinetti, A. Wasan, M. A. Bouchiat, A. V. Papoyan, and D. Sarkisyan, Phys. Rev. Lett. **90**, 143001 (2003); J. Guéna, M. Lintz, and M. A. Bouchiat, Phys. Rev. A **71**, 042108 (2005).
[25] M. A. Bouchiat, private communication.
[26] D. F. Kimball, Phys. Rev. A **63**, 052113 (2001).
[27] F. H. M. Faisal, *Theory of Multiphoton Processes* (Plenum Press, 1987).
[28] M. L. Ter-Mikaelyan, Physics - Uspekhi **40**, 1195 (1997).
[29] K. B. Blagoev and V. A. Komarovskii, Atomic Data and Nuclear Data Tables **56**, 1 (1994).
[30] S. G. Porsev, Y. G. Rakhlina, and M. G. Kozlov, Phys. Rev. A **60**, 2781 (1999).
[31] J. E. Stalnaker, D. Budker, D. P. DeMille, S. J. Freedman, and V. V. Yashchuk, Phys. Rev. A **66**, 031403 (2002).
[32] D. DeMille, Phys. Rev. Lett. **74**, 4165 (1995).
[33] V. A. Dzuba and V. V. Flambaum, Phys. Rev. A **83**, 042514 (2011).
[34] W. Demtröder, *Laser Spectroscopy*, 3rd ed. (Springer, 2003).
[35] S. Rochester, C. J. Bowers, D. Budker, D. DeMille, and M. Zolotorev, Phys. Rev. A **59**, 3480 (1999).
[36] A. Schäfer, G. Soff, P. Indelicato, B. Müller, and W. Greiner, Phys. Rev. A **40**, 7362 (1989).
[37] I. I. Sobelman, *Atomic Spectra and Radiative Transitions* (Springer-Verlag, 1992).
[38] D. A. Varshalovich, A. N. Moskalev, and V. K. Khersonskii, *Quantum Theory of Angular Momentum* (World Scientific, 1988).